Battery Aging, Battery Charging and the Kinetic Battery Model: A First Exploration

Marijn R. Jongerden[✉] and Boudewijn R. Haverkort

Design and Analysis of Communication Systems,
University of Twente, Enschede, The Netherlands
{m.r.jongerden,b.h.r.m.haverkort}@utwente.nl

Abstract. Rechargeable batteries are omnipresent and will be used more and more, for instance for wearables devices, electric vehicles or domestic energy storage. However, batteries can deliver power only for a limited time span. They slowly degrade with every charge-discharge cycle. This degradation needs to be taken into account when considering the battery in long lasting applications. Some detailed models that describe battery degradation processes do exist, however, these are complex models and require detailed knowledge of many (physical) parameters. Furthermore, these models are in general computationally intensive, thus rendering them less suitable for use in larger system-wide models. A model better suited for this purpose is the so-called Kinetic Battery Model. In this paper, we explore how this model could be enhanced to also cope with battery degradation, and with charging. Up till now, battery degradation nor battery charging has been addressed in this context. Using an experimental set-up, we explore how the KiBaM can be used and extended for these purposes as well, thus allowing for better integrated modeling studies.

Keywords: Kinetic battery model · Battery aging · Battery charging · Battery discharging · Measurements

1 Introduction

Batteries-powered devices are everywhere; smart-phones, laptops, wireless sensors, wearables, electric cars and for local energy storage. According to McKinsey, the Internet-of-Things (IoT) is expected to connect 1 trillion (10^{12}) devices by 2025, many of which will be battery powered. According to the International Energy Agency (IAE), in 2016, some 6.4% of Dutch cars was fully or hybrid electric; in Norway this was even 29%! Throughout 2016, the world's electric car population grew to 2 million cars, almost a doubling compared to the end of 2015. These developments clearly underline the importance of understanding battery charging and discharging, as well as battery degradation processes.

Batteries are needed to provide portable power to all these devices. However, batteries have a limited life span. Obviously, non-rechargeable batteries can be

discharged only once before they need to be replaced. But, even rechargeable batteries will not be usable after some time. How long a battery can be used depends on many factors, such as battery type, discharge and charge current, depth of discharge and temperature. It is hard to predict the lifetime of a battery for any given workload pattern. Electro-chemical and electrical circuit models, that require detailed knowledge of the used batteries, are available in the literature, see for example [1,2]. In recent work, Wognsen et al. [3] propose an approach to compare the impact workload patterns have on the battery life through the Fourier Transform of the workload.

Although some theoretical work exists, little practical work is available in the scientific literature on measuring battery degradation over time, and how such degradation effects models or model parameters. In this paper we present the results of an extensive measurement study on battery cells of the type are used in nano-satellites of GomSpace (lithium ion 18650 cells) [4], which are also used in Tesla electric vehicles [5]. These measurements are analyzed in the context of a widely used battery model, the Kinetic Battery Model. The analysis gives insight on how the degradation of the battery impacts the model parameters, and on how to possibly extend this model to cope with the effects of degradation. Furthermore, we also explicitly address the charging of such batteries; up till now, in the literature, it has been assumed that the charging process proceeds the same as discharging, with "just the flow of current flipped". We show that this is not exactly the case.

The rest of this paper is structured as follows. Section 2 gives a brief overview of related work on battery degradation modeling. Section 3 introduces the Kinetic Battery Model. In Sect. 4 the experimental set-up and the performed experiments are described. The results of the experiments are presented in Sect. 5 and discussed in Sect. 6. Section 7 concludes the paper.

2   Battery (Degradation) Models

There are several types of battery models available in the scientific literature. We provided an overview of the most widely used models, such as electro-chemical models, electrical circuit models and analytical models in [6], with a focus on predicting the duration of a single discharge cycle. These types of models are also used to describe the long-term effects of battery degradation.

In [1], so-called capacity fading is modeled with an electro-chemical battery model for a lithium-ion battery. This type of model requires a very detailed knowledge of the physical characteristics of the battery, and is computationally very intensive to use.

In [2] an electrical circuit model is made that models capacity fading due to cycling (repeated charge–discharge), as well as the increase of the internal resistance due to cycling. The model should be configured with data from the battery data sheets. However, as also the authors mention, in general, it is very hard to obtain all required parameters.

High-level analytical models, such as the Kinetic Battery Model (KiBaM) [7], require much less knowledge of the battery, and can be easily combined with

other models. For example, in [8], the KiBaM is extended to a random KiBaM and combined with a Markovian task process that models the battery load. With the combined model, one can compute the probability the battery is depleted due to the defined load pattern. The KiBaM, nor the proposed extensions, do take into account how the battery degrades; it is not known how the essential parameters are effected.

In [3], a generic method for comparing the impact of different load profiles on the wear of the battery is proposed. The load profiles are rated by analyzing the Fourier transform of the load. With this analysis different load profiles can be ranked from little impact on battery wear to large impact.
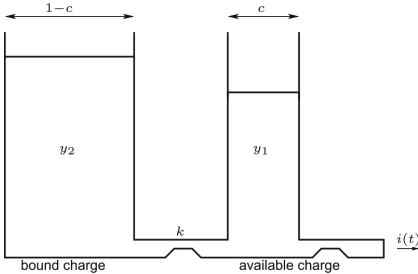

Fig. 1. The two-well Kinetic Battery Model.

However, it is not possible to quantify the wear with this method. In order to do this, many more measurements need to be performed. In this paper, we investigate how the KiBaM-parameters change when the battery is repeatedly discharged. We take an experimental approach. We wear the battery by applying a relatively heavy load to the battery. This gives us the practical insight in how the battery degrades over time.

3   The Kinetic Battery Model

The kinetic battery model (KiBaM) is a compact battery model that includes the most important features of batteries, i.e., the rate-capacity effect and the recovery effect. The model has been originally developed by Manwell and McGowan in 1993 [7] for lead-acid batteries, but analysis has shown that it can also be used in battery discharge modeling for other battery types [9].

3.1   Basic Dynamics

In the model, the battery charge is distributed over two wells: the *available-charge* well and the *bound-charge* well (cf. Fig. 1). A fraction c of the total capacity is considered to be in the available-charge well (denoted $y_1(t)$), and a fraction $1 - c$ in the bound-charge well (denoted $y_2(t)$). The available-charge well supplies electrons directly to the load $(i(t))$, whereas the bound-charge well supplies electrons only to the available-charge well. The charge flows from the bound-charge well to the available-charge well through a "valve" with fixed conductance, k. The parameter k has the dimension 1/time and limits the rate at which the charge can flow between the two charge wells. Next to this parameter, the rate at which charge flows between the wells depends on the height difference between the two wells. The heights of the two wells are given by: $h_1(t) = y_1(t)/c$

and $h_2(t) = y_2(t)/1 - c$. The change of the charge in both wells is given by the following system of differential equations:

$$\begin{cases} \dfrac{dy_1(t)}{dt} = -i(t) + k(h_2(t) - h_1(t)), \\ \dfrac{dy_2(t)}{dt} = -k(h_2(t) - h_1(t)), \end{cases} \quad (1)$$

with initial conditions $y_1(0) = c \cdot C$ and $y_2(0) = (1 - c) \cdot C$, where C is the total battery capacity. The battery is considered empty when it is observed that there is no charge left in the available-charge well. As shown in [9], we can transform the above equations to

$$\begin{cases} \dfrac{d\gamma(t)}{dt} = -i(t), \\ \dfrac{d\delta(t)}{dt} = \frac{1}{c}i(t) - k'\delta(t), \end{cases} \quad (2)$$

where $k' = k/(c(1 - c))$, $\gamma(t) = y_1(t) + y_2(t)$ and $\delta(t) = y_2(t)/(1 - c) - y_1(t)/c$. We can interpret $\gamma(t)$ as the total charge remaining in the battery, and $\delta(t)$ as the height difference between the the charge levels of the two wells. The initial conditions transform into $\gamma(0) = C$ and $\delta(0) = 0$. The battery is empty when $\gamma(t) = (1 - c)\delta(t)$.

3.2   KiBaM Constant Current Discharge

When we consider a constant current discharge, i.e., $i(t) = I_d$, the differential equations can easily be solved:

$$\begin{cases} \gamma(t) = C - I_d t, \\ \delta(t) = \dfrac{I_d}{ck'} \left(1 - e^{-k't}\right). \end{cases} \quad (3)$$

The battery lifetime L, i.e., the time to empty the available charge well, for a constant current discharge is given by:

$$L = \frac{C}{I_d} - \frac{1}{k'}\left(\frac{1-c}{c} + \mathcal{W}\left(\frac{1-c}{c}e^{\frac{1-c}{c} - \frac{Ck'}{I_d}}\right)\right), \quad (4)$$

where $\mathcal{W}(.)$ is the so-called Lambert $\mathcal{W}$ function [10]. By measuring the battery lifetime, and the delivered energy, as a function of the discharge current, we can determine the KiBaM parameters k, c and C by fitting (4) to the data.

3.3   KiBaM Charging

Battery charging normally is performed in two phases. First, the battery is charged at a constant current. In this phase the voltage will slowly rise. When the voltage reaches the maximum level, V_{max}, the second phase starts, during which the voltage is kept constant at V_{max} and the charging current will drop. We discuss the two charging phases in the context of the KiBaM model in the following sections.

KiBaM Constant Current Charging. In the KiBaM, the charging with a constant current is very similar to discharging with a constant current. For a constant charging current I_{ch} the KiBaM equations are:

$$\begin{cases} \frac{dy_1(t)}{dt} = I_{ch} - k\left(\frac{y_1(t)}{c} - \frac{y_2(t)}{1-c}\right), \\ \frac{dy_2(t)}{dt} = k\left(\frac{y_1(t)}{c} - \frac{y_2(t)}{1-c}\right). \end{cases} \tag{5}$$

When we consider the battery fully empty at the start of the charging, the initial conditions are $y_1(0) = 0$ and $y_2(0) = 0$. The constant current charging phase ends when the available charge well is filled, thus $y_1 = cC$. In terms of $\delta_{ch}(t) = \frac{y_1(t)}{c} - \frac{y_2(t)}{1-c}$ ($\delta_{ch}(t) = -\delta(t)$) and $\gamma(t) = y_1(t) + y_2(t)$, the equations are:

$$\begin{cases} \frac{d\gamma(t)}{dt} = I_{ch}(t), \\ \frac{d\delta_{ch}(t)}{dt} = \frac{I_{ch}(t)}{c} - k'\delta_{ch}(t), \end{cases} \tag{6}$$

The initial conditions transform into $\delta_{ch}(0) = 0$ and $\gamma(0) = 0$. The condition for the end of the constant current charging phase is $\gamma(t_{lin}) + (1-c)\delta_{ch}(t_{lin}) = C$. This condition can be interpreted as follows, at time $t = t_{lin}$, the amount of energy put into the battery is $\gamma(t_{lin})$ and still $(1-c)\delta_{ch}(t_{lin})$ needs to be charged. The solutions for $\gamma(t)$ and $\delta_{ch}(t)$ are again easily obtained:

$$\begin{cases} \gamma(t) = I_{ch}t, \\ \delta_{ch}(t) = \frac{I_{ch}}{ck'}(1 - e^{-k't}), \end{cases} \tag{7}$$

where we see that the equation for δ is the same as for discharging, cf. (3).

Under the above described conditions, the time it takes to fill the available charge well, t_{lin}, is similar to the discharging lifetime, cf. (4):

$$t_{lin} = \frac{C}{I_{ch}} - \frac{1}{k'}\left(\frac{1-c}{c} + \mathcal{W}\left(\frac{1-c}{c} \cdot e^{\frac{1-c}{c} - \frac{Ck'}{I_{ch}}}\right)\right). \tag{8}$$

We can estimate the charging parameters by measuring the duration of the linear charging phase for different charge currents, and fitting the equation to the results.

KiBaM Non-linear Charging. After the linear charging phase, the battery is charged with a constant voltage and a decreasing current. In the KiBaM we can interpret this as follows. The constant voltage keeps the level of the available charge at its maximum. The rate at which the battery can accept additional charge is limited by the flow between the two charge wells. This rate depends on the height difference between the two wells, and thus will decrease when the battery is further charged.

Since the available charge does not change, we have $\frac{dy_1(t)}{dt} = 0$. From the KiBaM equations we therefore obtain:

$$i(t) = k\left(\frac{y_1(t)}{c} - \frac{y_2(t)}{1-c}\right). \tag{9}$$

In terms of $\delta_{ch}(t) = \frac{y_1(t)}{c} - \frac{y_2(t)}{1-c}$ this yields:

$$i(t) = k\delta_{ch}(t) = k'c\,(1-c)\,\delta_{ch}(t). \tag{10}$$

The KiBaM equations in terms of $\delta_{ch}(t)$ and $\gamma(t)$ now are,

$$\begin{cases} \frac{d\gamma(t)}{dt} & = i(t) = k'c(1-c)\delta_{ch}(t), \\ \frac{d\delta_{ch}(t)}{dt} & = \frac{i(t)}{c} - k'\delta ch(t) = -k'c\delta_{ch}(t), \end{cases} \tag{11}$$

From these equations it follows that

$$\delta(t) = \delta_0 e^{-ck't}, \tag{12}$$

where δ_0 is the height difference between the two wells at the start of the non-linear charging phase (I_{lin}); δ_0 depends on the charging current in the linear phase. From Eqs. (7) and (8) it follows that

$$\delta_0 = \frac{I_{lin}}{ck'}\left(1 - e^{-ck't_{lin}}\right). \tag{13}$$

If $k't_{lin}$ is large, that is, if the height difference has approached its maximum value during the linear charging phase, we obtain

$$\delta_0 = \frac{I_{lin}}{ck'}. \tag{14}$$

The height difference decreases exponentially, and thus the charging current should decrease exponentially. By fitting an exponential function to the measured current we can estimate the factor ck'. This gives additional information on how the KiBaM performs for charging the battery.

4   Experimental Set-Up

In the experiments we analyze 4 lithium-ion battery cells with a capacity of 2600 mAh, obtained from GomSpace (www.gomspace.com). The nano-satelite battery packs consist of 4 to 8 of these battery cells. Table 1 gives an overview of the key parameters, as provided in the datasheets.

Table 1. Parameters of the GomSpace lithium-ion batteries [4]

Parameter	Value
Nominal capacity	2600 mAh
Maximum charge voltage	4.2 V
End of discharge voltage	3.0 V
Maximum discharge current	3.75 A
Maximum charge current	2.5 A
End of charge current	1.3 A
Charge temperature range	-5–$45\,^{\circ}$C
Discharge temperature range	-20–$60\,^{\circ}$C

The measurements are performed with the Cadex C8000 battery testing system, cf. Fig. 2, which can test four batteries simultaneously. The tester is programmed to discharge and charge the cells in a controlled fashion according to a user-defined load profile, while measuring the voltage, current and temperature. This data is logged each second, and is used for the analysis of the battery properties. The experiments are conducted in a number of steps (phases):

1. In the first phase, *KiBaM estimation measurements*, the cells are discharged and charged at various constant rates. The charge rates vary from 0.1 C to 0.9 C, while the discharge rates vary from 0.1 C to 1.4 C. Table 2 gives an overview of the discharge and charge currents of the individual measurement cycles. The data from these measurements will be used to estimate the parameters for the Kinetic Battery Model.
2. In the second phase, *the degradation measurements*, the cells are repeatedly fully discharged at 1 C and charged at 0.5 C. This high load will result in
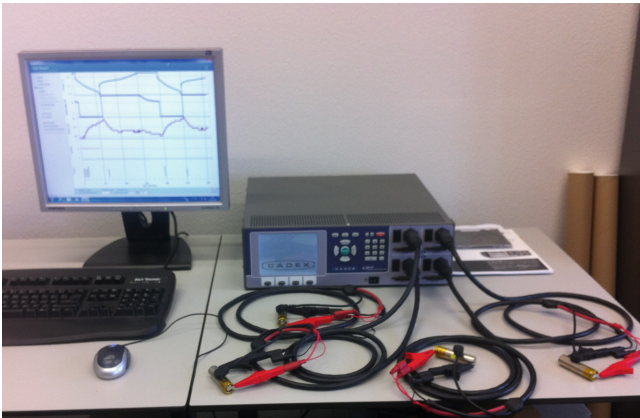

Fig. 2. Experimental set-up with the Cadex C8000 battery tester.

Table 2. Discharge and charge currents for the parameter estimation measurements.

Test	Discharge current	Charge current	Test	Discharge current	Charge current
1	$0.1\,\mathrm{C} = 0.26\,\mathrm{A}$	$0.1\,\mathrm{C} = 0.26\,\mathrm{A}$	7	$0.7\,\mathrm{C} = 1.82\,\mathrm{A}$	$0.7\,\mathrm{C} = 1.82\,\mathrm{A}$
2	$0.2\,\mathrm{C} = 0.52\,\mathrm{A}$	$0.2\,\mathrm{C} = 0.52\,\mathrm{A}$	8	$0.8\,\mathrm{C} = 2.08\,\mathrm{A}$	$0.8\,\mathrm{C} = 2.08\,\mathrm{A}$
3	$0.3\,\mathrm{C} = 0.78\,\mathrm{A}$	$0.3\,\mathrm{C} = 0.78\,\mathrm{A}$	9	$0.9\,\mathrm{C} = 2.34\,\mathrm{A}$	$0.9\,\mathrm{C} = 2.34\,\mathrm{A}$
4	$0.4\,\mathrm{C} = 1.04\,\mathrm{A}$	$0.4\,\mathrm{C} = 1.04\,\mathrm{A}$	10	$1.0\,\mathrm{C} = 2.60\,\mathrm{A}$	$0.6\,\mathrm{C} = 1.56\,\mathrm{A}$
5	$0.5\,\mathrm{C} = 1.3\,\mathrm{A}$	$0.5\,\mathrm{C} = 1.3\,\mathrm{A}$	11	$1.2\,\mathrm{C} = 2.86\,\mathrm{A}$	$70.7\,\mathrm{C} = 1.82\,\mathrm{A}$
6	$0.6\,\mathrm{C} = 1.56\,\mathrm{A}$	$0.6\,\mathrm{C} = 1.56\,\mathrm{A}$	12	$1.4\,\mathrm{C} = 3.64\,\mathrm{A}$	$70.9\,\mathrm{C} = 2.34\,\mathrm{A}$

    a relative fast degradation of the cells. After 50 discharge-charge cycles, the cycles of the first phase are repeated, in order to see whether and how the battery parameters have changed.

3. The battery parameters will be determined after every such 50 repetitions, until the cell capacity has dropped below 80% of its initial value. The results of these experiments give an indication on how the cells degrade over time.

5   Measurement Results

In this section we discuss the results of the performed measurements. We start with the degradation measurements in Sect. 5.1, since these results provide a clear view on how the battery slowly degrades during the experiments. Then, we analyze the change of the KiBaM parameters for discharging and charging in Sects. 5.2 and 5.3, respectively.

5.1   Degradation Measurements

Figure 3 shows how the discharge capacity decreases as a function of the discharge cycle number. In the first discharge cycle, on average, the batteries deliver 92.8% of the nominal capacity (2600 Ah). In the subsequent cycles the discharge capacity slowly drops. The decrease in capacity is more or less linear. We fit a linear function, $Cap^{(1-100)} = \alpha \cdot cycle + \beta$, to the first 100 measurements with using the nonlinear least squares method built in the Matlab fit function. The fit yields the following estimates and 95% confidence intervals: $\alpha = -0.057 \pm 0.0025$ and $\beta = 92.8 \pm 0.14$. This means that the capacity, on average, drops 0.057% point with every discharge-charge cycle.

    After approximately 140 cycles the capacity decreases more rapidly. Battery 3 (yellow) now degrades clearly faster than the other 3 batteries. We fit another line, $Cap^{(151-200)} = \alpha \cdot cycle + \beta$, to the last 50 measurements, cycle 151 to 200. This yields, $\alpha = -0.41 \pm 0.027$ and $\beta = 144.2 \pm 4.8$. This means that the degradation is more than a factor 7 faster than in the first phase, with an average of 0.41% point per cycle.
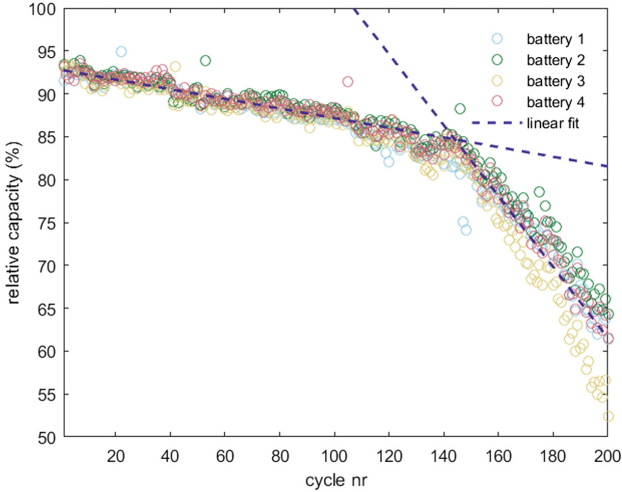
Fig. 3. Capacity relative to the nominal capacity as a function of the cycle number. (Color figure online)

Next to the capacity we investigate how the efficiency evolves when the battery is used. The efficiency, in percent, is determined as $100 \cdot E_{dis,n}/E_{ch,n-1}$, where $E_{dis,n}$ is the delivered energy in cycle n, and $E_{ch,n-1}$ is the charging energy of cycle $n-1$. The results are shown in Fig. 4. As for the capacity, we see that the efficiency also degrades in two phases. Again we fit two lines to the data. The first line is fit to the first 100 cycles. The efficiency starts at $89.3\% \pm 0.17$. The efficiency degrades linearly with a rate of $0.020 \pm 0.0028\%$ point per cycle. The second line is fit to the last 50 cycles. Here we see that the efficiency degrades at a rate of $0.061 \pm 0.022\%$ point per cycle. This means that the efficiency degrades 3 times faster at the end of the battery life than at the beginning. Furthermore, we see that the variation of the measured efficiency is much larger at the end of the battery lifetime.

Finally, we investigate the non-linear charge phase of the degradation measurements. According to the KiBaM theory, the charge current should drop exponentially during the non-linear charge phase, cf. Eq. (12). We fit a negative exponential curve to the measured current. In Fig. 5, the exponent, which corresponds to $k'c$, is plotted as a function of the cycle number. We see that the exponent decreases as the number of discharge-charge cycles increases. We have fitted a linear curve, $y = \alpha \cdot x + \beta$ to the data. This fit yields $\alpha = -1.71 \cdot 10^{-6} \pm 0.05 \cdot 10^{-6}$ and $\beta = 1.03 \cdot 10^{-3} \pm 0.005 \cdot 10^{-3}$. In the KiBaM, the decrease of the exponent $k'c$ is either caused by a decrease in k, i.e., the conductance between the available and bound charge well, or by a decrease in c, i.e., the size of the available charge well. The slower exponential drop of the charging current may also be a result of the drop in the charging efficiency, which we discussed above. The charging efficiency, however, is currently not included in the KiBaM.
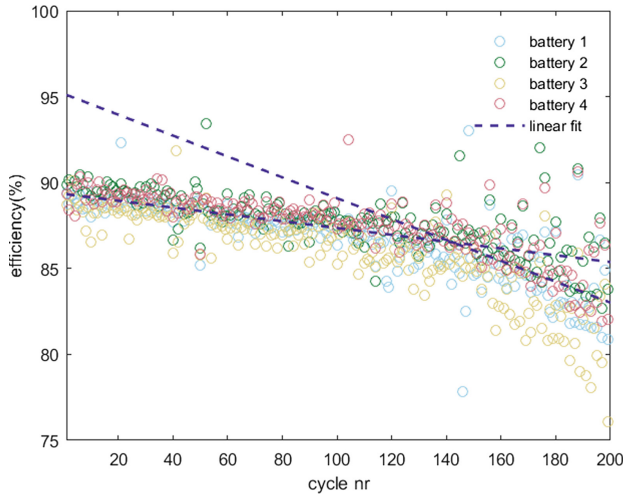
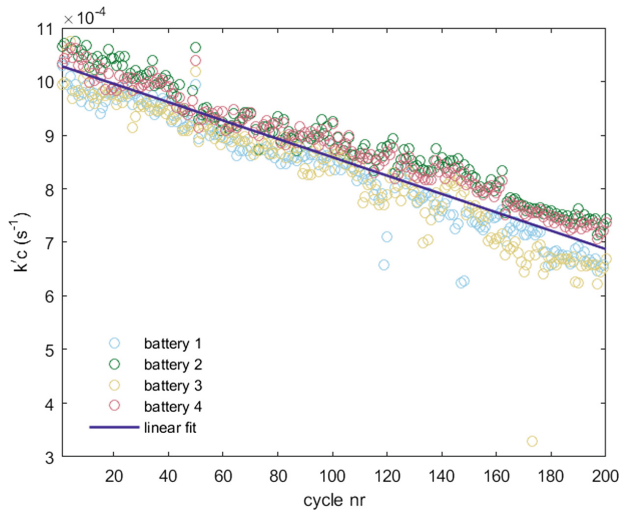**Fig. 4.** Efficiency of charge discharge cycle as a function of the cycle number.

Fig. 5. The exponent for the non-linear charge phase as a function of the cycle number.

5.2 KiBaM Discharging Parameter Estimation

We started the battery degradation analysis with a series of measurements for determining the KiBaM parameters. In these measurements the batteries are discharged and charged at various constant currents, cf. Table 2. These measurements have been repeated after every 50 cycles in the degradation measurements. Figure 6(a) shows the measured discharge capacity of the four batteries for the different discharge currents of the first series.

The measurements at $0.9\,C = 2.34$ A discharging current have been performed twice. The first run, which was the first experiment that was performed, resulted for all batteries in a discharge capacity that was higher than expected. The second run resulted in a capacity that was in line with the other experiments. The reason for these results remains unclear.

For battery 3, we see a relative low capacity at the low discharge currents. We expect that this is due to some internal damage or lower quality of the battery. Battery 3 has a slightly lower performance throughout the experiments, as we will see in the later results.

The measured delivered capacity (C_{del}) in As as a function of the discharge current (I_d) is fitted to the function (cf. 4):

$$C_{del} = C_{nom} - \frac{I_d}{k'} \left(\frac{1-c}{c} + \mathcal{W} \left(\frac{1-c}{c} e^{\frac{1-c}{c} - \frac{C_{nom}k'}{I_d}} \right) \right)$$ (15)

In the fitting procedure we use the parameter $\kappa = 1/k'$ instead of k', since the fitting algorithm was not stable when k' was used directly. In the fit we ignored the outliers of the first measurement and battery 3. The result is included in Fig. 6(a). From the fit we obtained $C = 9.67 \cdot 10^3 As \pm 220\ As$, which is higher than the nominal capacity of 2600 mAh = 9360 As. The other parameters are: $c = 0.90 \pm 0.015$ and $\kappa = 9.36 \cdot 10^3 s \pm 9.12 \cdot 10^3 s$. The parameter κ has a very large confidence interval, thus we cannot draw any strong conclusions on the actual value of this parameter, nor for the parameter $k = 1/\kappa$.

After every 50 discharge-charge cycles another series of measurements is done to determine the KiBaM parameters. The results are given in Figs. 6(b)–(e). In these figures we see that, like in the degradation measurements, the capacity first drops slowly in Figs. 6(b) to 6(d), and then drops dramatically in Fig. 6(e). In all these measurement series, as in the results of the first series, battery 3 shows a lower capacity for the low discharge currents. At high discharge currents, i.e., larger than 2.5 A, all batteries perform less good than expected. When we include these measurements in the fitting procedure the results for the parameters c and κ are nearly meaningless, with extremely large confidence intervals. The degradation of the battery clearly has a larger impact when high discharge currents are applied.

When we discard the high current measurements in the fitting procedure, the results are more in line with the analysis of the first measurement series (cf. Sect. 5.2). The values of the fitted parameters and their confidence intervals are given in Table 3(a). We see a decrease in the capacity of the battery, as expected. Also, the parameter c slowly decreases, as the battery ages. This means that the decrease in capacity affects the available charge more than the bound charge. For the parameter κ it is, statistically speaking, impossible to tell whether the battery degradation has any real impact, due to the large confidence intervals.
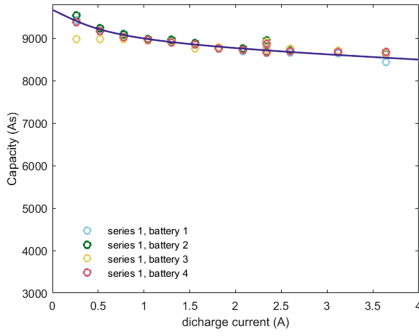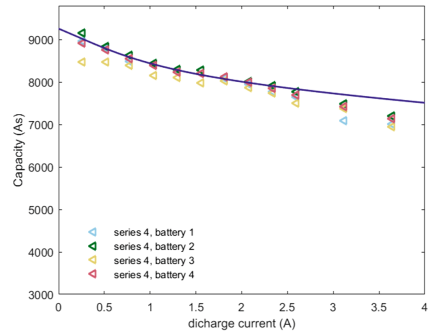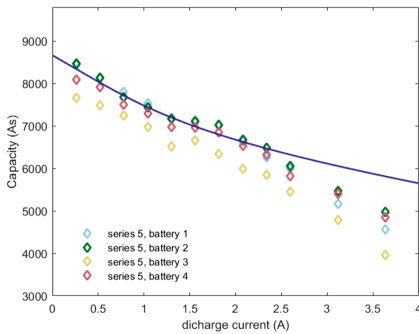
(a) series 1
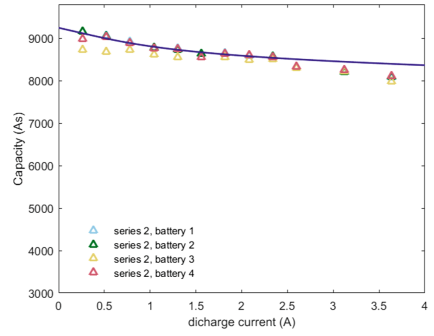
(b) series 2
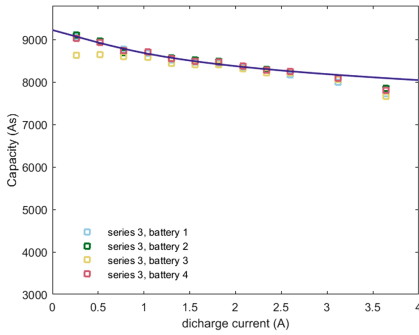
(c) series 3

(d) series 4

(e) series 5

Fig. 6. Measured discharge capacity as function of the discharge currents and a non-linear least squares fit of the KiBaM for the 5 measurements series.

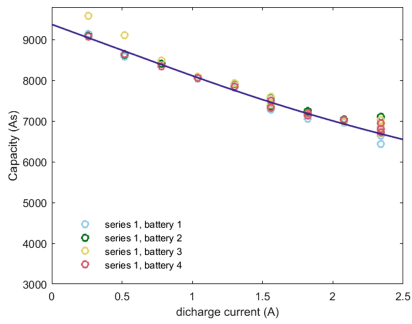### 5.3   KiBaM Charging Parameter Estimation

Next to the parameters for discharging, we also fit the KiBaM parameters to the charging measurements. Figure 7 shows the energy put into the battery during the linear charge phase of the five series. In all five figures we notice some deviating measurements. These measurements coincide with the deviations in the discharge results. Battery 3 again deviates at low currents, however, the linear charge capacity is larger than for the other batteries at low currents, whereas the discharge capacity was lower.

Table 3. KiBaM parameters and the 95% confidence intervals based on a non-linear least squares fit of the (a) discharge measurements (upper half), and (b) charge measurements (lower half).
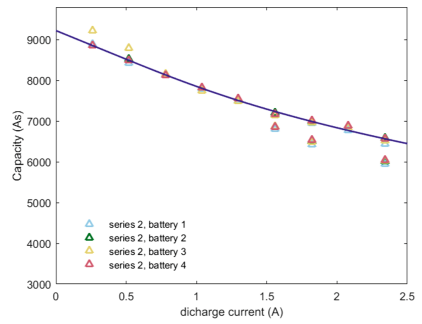
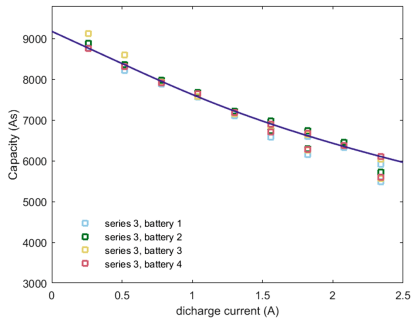| Experiment	$C(10^3$ As$)$	c	κ $(10^3$ s$)$
(a) Discharge measurements			
Series 1	9.67 ± 0.22	0.90 ± 0.015	9.36 ± 9.12
Series 2	9.25 ± 0.10	0.90 ± 0.019	4.37 ± 2.66
Series 3	9.23 ± 0.08	0.86 ± 0.019	3.76 ± 1.56
Series 4	9.26 ± 0.15	0.83 ± 0.027	4.43 ± 2.24
Series 5	8.67 ± 0.26	0.70 ± 0.080	2.85 ± 2.05
(b) Charge measurements			
Series 1	9.38 ± 0.12	0.579 ± 0.076	1.74 ± 0.73
Series 2	9.22 ± 0.09	0.646 ± 0.031	2.57 ± 0.59
Series 3	9.18 ± 0.12	0.599 ± 0.045	2.37 ± 0.70
Series 4	9.09 ± 0.15	0.548 ± 0.057	2.22 ± 0.78
Series 5	8.57 ± 0.27	0.504 ± 0.071	2.62 ± 1.21

The outliers are again discarded in the fitting procedure. The curves we fitted are given in Fig. 7, and the parameters are given in Table 3(b). Again, we see that the capacity decreases. The estimated capacity is, however, smaller than for discharging. The parameter c is much smaller during charging than during discharging. This implies that the available charge well is much smaller when the battery is charged. For the parameter κ it is again hard to draw firm conclusions. The estimated values for κ are lower for charging than for discharging. This suggests that t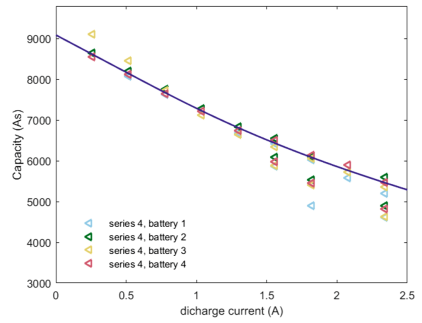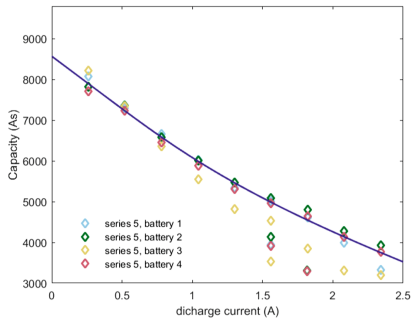he flow between bound and available charge is faster during charging than during discharging. It difficult to interpret the differences between the KiBaM parameters for discharging and charging within the context of the chemical battery processes. However, our experiments do show that when the KiBaM model is used, it appears **not justified** to just reverse the flow of the current and keep the parameters the same when we switch from discharging to charging.

Fig. 7. Measured linear charge capacity as function of the charge currents and a non-linear least squares fit of the KiBaM for the 5 measurements series.

6   Discussion

The measurements do bring forward three main points for improvements of the KiBaM. First of all, the KiBaM does not take into account the efficiency, ϵ, of the battery. This may be corrected by multiplying the charge current with a factor ϵ in the KiBaM equations for charging, cf. Eq. (5). This correction will account all losses to the charging process. In an equivalent manner, all losses can be accounted to the discharging process by multiplying the discharge current with $1/\epsilon$. Since it is not possible to determine the efficiency of charging and discharging process separately either solution, or a mix, is valid.

The second improvement of the KiBaM is to use different parameters c and k for charging and discharging. In the analysis we see that the parameter c is clearly larger for discharging. One challenge in changing the parameter c, when switching from charging to discharging, and vice versa, is how to redistribute the charge in the battery over the available and bound charge wells. Since the KiBaM model actually is a first order approximation of the continuous diffusion model by Rakhmatov and Vrudhula [9,11], the most natural option seems to be to keep the height of the available charge well constant, and redistribute the charge accordingly. Due to the large confidence intervals for the parameter k, we cannot draw any strong conclusions on how this parameter should change between charging and discharging. However, changing this parameter can be done without any additional challenges arising.

The third improvement to the KiBaM model deals with the battery degradation. The experiments show a degradation of the capacity and efficiency of the battery, as well as a change in the parameter c, both for charging and discharging. It is not straightforward how to incorporate the degradation into the KiBaM. As stated earlier, the rate of the battery degradation highly depends on the discharge and charge rate and the depth of discharge. Since the degradation is a slow process, one can use the KiBaM with constant parameters when considering a time scale of a couple of charge-discharge cycles. However, when the battery is modeled over a longer period, the degradation must be taken into account. This might be done with a multi-modal KiBaM, in which one switches between different constant parameter sets as the battery degrades. In order to know when to change parameter sets, more experiments are needed, in which the batteries are discharged at various rates and to different depths of discharge.

Finally, our experiments clearly show the degradation of the battery over time. Note that in the experiments we applied a relatively heavy load to the battery, by discharging it fully in just one hour. Both this high discharge rate and discharging to a very low state of charge have a negative impact on the overall battery lifetime [3]. In most practical scenarios, a battery will not be discharged at such high rates nor to such a low state of charge. Commercial devices often discharge lithium-ion batteries only to 20% state of charge, in order to preserve the battery. In order to translate the measured degradation to a practical scenario further measurements and analysis are needed.

7 Conclusion

In this paper we presented the results of a first experimental analysis of the aging process for a set of lithium-ion 18650 cells. In the analysis we see that these batteries degrade in two phases. In the first phase, of approximately 140 cycles, the capacity drops slowly at a rate of 0.057% point with every cycle. In the second phase the degradation increases with a factor 7. Next to measuring the degradation of the battery, we also estimated the KiBaM parameters at several points during the degradation process, in order to learn how the parameters change as the battery ages. Furthermore, our experiments show that the KiBaM parameters are different for charging and discharging. The analysis resulted in a number of proposals on how to extend the KiBaM to take into account the results of the experiments. We do note, however, that more experimental work is needed, with different workload scenarious and battery types, to make more concrete proposals for such model extensions.

References

1. Ning, G., Popov, B.N.: Cycle life modeling of lithium-ion batteries. J. Electrochem. Soc. **151**(10), A1584–A1591 (2004)
2. Petricca, M., Shin, D., Bocca, A., Macii, A., Macii, E., Poncino, M.: Automated generation of battery aging models from datasheets. In: Proceedings of the 32nd IEEE International Conference on Computer Design (ICCD), pp. 483–488. IEEE (2014)
3. Wognsen, E.R., Haverkort, B.R., Jongerden, M., Hansen, R.R., Larsen, K.G.: A score function for optimizing the cycle-life of battery-powered embedded systems. In: Sankaranarayanan, S., Vicario, E. (eds.) FORMATS 2015. LNCS, vol. 9268, pp. 305–320. Springer, Cham (2015). doi:10.1007/978-3-319-22975-1_20
4. GomSpace: NanoPower Battery Datasheet, Lithium Ion 18650 cells for space flight products (2012) supplied by GomSpace (2015)
5. Berdichevsky, G., Kelty, K., Straubel, J., Toomre, E.: The Tesla roadster battery system. Tesla Motors **1**(5), 1–5 (2006). http://large.stanford.edu/publications/coal/references/docs/tesla.pdf
6. Jongerden, M.R., Haverkort, B.R.: Which battery model to use? IET Softw. **3**(6), 445–457 (2009)
7. Manwell, J.F., McGowan, J.G.: Lead acid battery storage model for hybrid energy systems. Sol. Energy **50**(5), 399–405 (1993)
8. Hermanns, H., Krčál, J., Nies, G.: Recharging probably keeps batteries alive. In: Berger, C., Mousavi, M.R. (eds.) CyPhy 2015. LNCS, vol. 9361, pp. 83–98. Springer, Cham (2015). doi:10.1007/978-3-319-25141-7_7
9. Jongerden, M.R.: Model-based energy analysis of battery powered systems. Ph.D. thesis, University of Twente, Enschede, December 2010
10. Wolfram Mathworld (2015). http://mathworld.wolfram.com/LambertW-Function.html. Accessed November 2016
11. Rakhmatov, D.N., Vrudhula, S.B.K.: An analytical high-level battery model for use in energy management of portable electronic systems. In: Proceedings of the 2001 IEEE/ACM International Conference on Computer-Aided Design, ICCAD 2001, 488–493. IEEE Press, Piscataway (2001)